Sealing of Anodized Aluminum Alloys with Rare Earth Metal Salt Solutions

F. Mansfeld,*,[a] C. Chen,,[a] C. B. Breslin,***,[b] and D. Dull[c]**

[a]*Department of Materials Science and Engineering, University of Southern California, Los Angeles, California 90089-0241, USA*
[b]*Department of Chemistry, National University of Ireland, Maynooth, Ireland*
[c]*Boeing Information, Space and Defense Systems, Seattle, Washington 98124-2499, USA*

ABSTRACT

Boric-sulfuric acid anodized (BSAA) aluminum alloys have been sealed in hot solutions of cerium or yttrium salts. For comparison, sealing has also been performed in the presently used dilute chromate solution, boiling water, and a cold nickel fluoride solution. The corrosion resistance of the sealed BSAA Al alloys Al 2024, Al 6061, and Al 7075 has been evaluated by recording impedance spectra during exposure in 0.5 N NaCl for 7 days. Shorter or longer exposure times have also been used depending on the corrosion resistance obtained by different sealing processes. From the impedance spectra the time dependence of the pore resistance, R_{po}, and the specific admittance, A_s, has been determined. At the end of the exposure the pitted area, A_{pit}, was calculated. The relationship between A_s and R_{po} has been evaluated. Two different sealing mechanisms were detected. For sealing in dilute chromate the pores in the outer oxide layer stayed open, while for hot water sealing or sealing in cold nickel fluoride the pores were closed by an oxide/hydroxide. Sealing of BSAA Al alloys in cerium or yttrium salt solutions occurred according to one of these two mechanisms depending on alloy type and solution composition. Based on the experimental values of R_{po}, A_s, and A_{pit} it was concluded that sealing in cerium nitrate and yttrium sulfate solutions provided corrosion resistance similar to that of chromate-sealed BSAA Al alloys.

Introduction

Oxide layers on aluminum alloys produced by anodizing are commonly sealed in order to improve their corrosion resistance. Sealing of anodized aluminum has recently been reviewed by Yaffe,[1] who covered methods such as sealing in steam and hot water, nickel acetate, chromate, and various cold sealing methods. Some of the newer sealing methods have been developed due to environmental concerns and the desire to lower costs. Cold sealing in nickel fluoride has been introduced in order to lower these costs.[2-4] Chromate sealing suffers from the fact that chromates are confirmed human carcinogens. Recently, health hazards have also been observed for nickel salts which can cause allergic contact dermatitis.[5] Various alternative sealing processes have therefore been introduced. A process in which chromic acid is replaced as the anodizing solution by sulfuric acid and sealing is carried out at lower temperatures in nickel acetate instead of sodium dichromate has been described.[6] This process produced thinner anodized layers with improved fatigue properties but did not address the health hazards due to the use of nickel salts. A comparison of results obtained with some of these alternative sealing processes and sealing in cerium acetate has recently been performed for Al 2024, Al 6061, and Al 7075.[7] In Boeing's boric-sulfuric acid anodize (BSAA) process anodized layers of about 1 μm thickness are produced, which are sealed in a dilute chromate solution.[8]

Treatment of commercial aluminum alloys in rare earth metal salt (REMS) solutions has produced surfaces with excellent resistance to pitting.[9-11] For Al 2024 and Al 7075 a pretreatment step has been used to remove copper from the outer surface layers.[12] Some of these REMS solutions have been evaluated as nonchromate sealing procedures for Al 2024, Al 6061, and Al 7075, which find wide use in the aerospace industry.[13] These alloys were anodized with the BSAA process.[8] The corrosion resistance of the resulting anodized layers has been determined during exposure to 0.5 N NaCl using electrical impedance spectroscopy (EIS). Samples sealed with the most promising REMS solutions have been subjected to paint adhesion and salt spray testing at Boeing.

Experimental

Materials and methods.—Materials.—Boric-sulfuric acid anodized (BSAA) Al 2024-T3, Al 6061, and Al 7075-T6 samples were received from Boeing Space and Defense Group. The anodizing solution contained 45 mg/L sulfuric acid and 8 mg/L boric acid.[8] One set of samples had been sealed in a dilute (45 ppm Cr^{6+}) chromate solution; the others had not been sealed. From the experimental coatings weights for BSAA Al 2024, Al 6061, and Al 7075 oxide thicknesses of 0.67, 1.27, and 1.07 μm, respectively, were obtained. The BSAA oxides were thinner than those obtained by conventional sulfuric anodizing where oxides of about 20 μm are formed.

Sample preparation.—The as-received samples were cleaned with alconox, degreased in hexane, rinsed in deionized water, and then air dried. For sealing, the BSAA samples were immersed in the sealing solution (temperature and pH depending on the particular sealing processes) for the specified time period. After removing the sample from the sealing solution, it was rinsed thoroughly with deionized water and then air dried.

Sealing procedures.—The BSAA Al alloys were sealed in hot water, cold nickel fluoride, and different cerium and yttrium salt solutions. Hot water sealing (HWS) was carried out in boiling deionized water for 15 min. In cold NiF_2 sealing, the samples were immersed in 5 g/L $NiF_2 \cdot 4H_2O$, pH 6 solution at 25°C for 15 min, then aged in boiling water for 1 min. The different cerium salts included cerium acetate, cerium nitrate, cerium(III), and cerium(IV) sulfate. Yttrium acetate, yttrium chloride, and yttrium sulfate were the yttrium salts used. The cerium or yttrium concentration, pH values, and sealing times were varied in the different sealing processes.[13]

Cerium acetate sealing was carried out in boiling 5 mM $Ce(CH_3COO)_3$ solution for 30 min. Cerium nitrate I and II sealing was performed in boiling 50 mM $Ce(NO_3)_3$ for 15 or 30 min, respectively. In a process in which sealing in cerium acetate was followed by cerium nitrate sealing, the samples were sealed in boiling 5 mM $Ce(CH_3COO)_3$ solution for 10 min followed by sealing in boiling 50 mM $Ce(NO_3)_3$ for 10 min. In cerium(III) sulfate sealing, the samples were immersed in boiling 50 mM $Ce_2(SO_4)_3$ solution (pH adjusted to 5.4) for 15 min. Sealing in the two cerium(IV) sulfate I and II solutions was performed for 30 min in boiling 25 or 50 mM $Ce(SO_4)_2$ solution at a pH of 5.4 or 6, respectively.

In the yttrium chloride sealing process, the samples were sealed in boiling 15 mM YCl_3 solution for 15 min. For sealing in yttrium acetate, the samples were immersed in boiling 50 mM $Y(CH_3COO)_3$ solution (pH adjusted to 5.14) for 15 min. The two yttrium sulfate I and II sealing processes were carried out in boiling 25 mM $Y_2(SO_4)_3$ solution (pH

* Electrochemical Society Fellow.
** Electrochemical Society Student Member.
*** Electrochemical Society Active Member.

Downloaded on 2017-02-21 to IP 149.157.61.151 address. Redistribution subject to ECS terms of use (see ecsdl.org/site/terms_use) unless CC License in place (see abstract).

adjusted to 5.28) for 15 min or in 50 mM $Y_2(SO_4)_3$ solution (pH adjusted to 6) for 30 min.

Methods.—Sealed BSAA samples were immersed in 0.5 N NaCl solution (open to air) and the sealing quality was evaluated by recording impedance spectra at the corrosion potential E_{corr}. The immersed area was 20 cm^2. The impedance spectra were analyzed with the ANODAL software[14] or with the PITFIT[14,15] software if pitting occurred. Samples were usually removed after 7 days immersion. Some tests for samples with exceptional corrosion resistance were extended to 14 days. The samples were visually observed throughout the immersion period. After the samples were removed, they were observed in an optical microscope at a magnification of 30 times. The number of pits was determined and the pitted area A_{pit} was estimated.

Results and Discussion

Since Al 2024 is the most difficult alloy in terms of efficient corrosion protection, impedance spectra are shown for this alloy to illustrate the results obtained for samples anodized in the BSAA process and sealed in boiling water, dilute chromate, and cold nickel fluoride in Fig. 1. The two time constants observed for HWS BSAA Al 2024 correspond to the inner and outer oxide layer produced by anodizing. The decrease of the impedance with exposure time is due to dissolution of the outer oxide layer (Fig. 1a). The changes of the impedance spectra at the lowest frequencies indicate pit initiation after about 1 day immersion.[9,10,14,15] The very stable impedance spectra for chromate-sealed Al 2024 reflect its excellent corrosion resistance (Fig. 1b). Only one time constant was observed since the pores in the oxide were not closed by a hydrated oxide. The capacitance determined for sealing in chromate corresponded to that of the inner barrier layer of about 100 Å thickness ($\epsilon_b = 10$).[7] For sealing in cold nickel fluoride (Fig. 1c), two time constants were observed in the impedance spectra indicating that the pores in the oxide layer were sealed with hydroxide similar to HWS.[7] The impedance spectra were quite stable with time and very few pits were found after 1 week immersion.

Figure 2 gives the impedance spectra for BSAA Al 2024, Al 6061, and Al 7075 sealed in cerium nitrate for 30 min. The impedance spectra for Al 6061 and Al 7075 clearly showed two time constants throughout the entire immersion period indicating that the pores in the outer porous

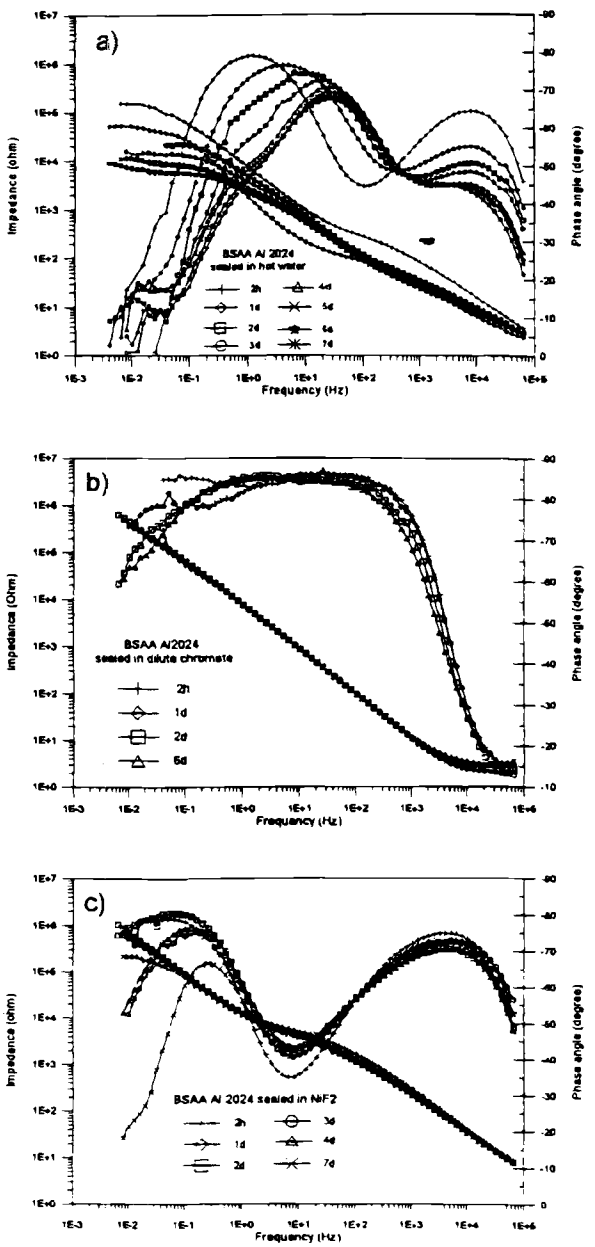

Fig. 1. Impedance spectra for BSAA Al 2024 sealed in (a) hot water, (b) dilute chromate, and (c) nickel fluoride.

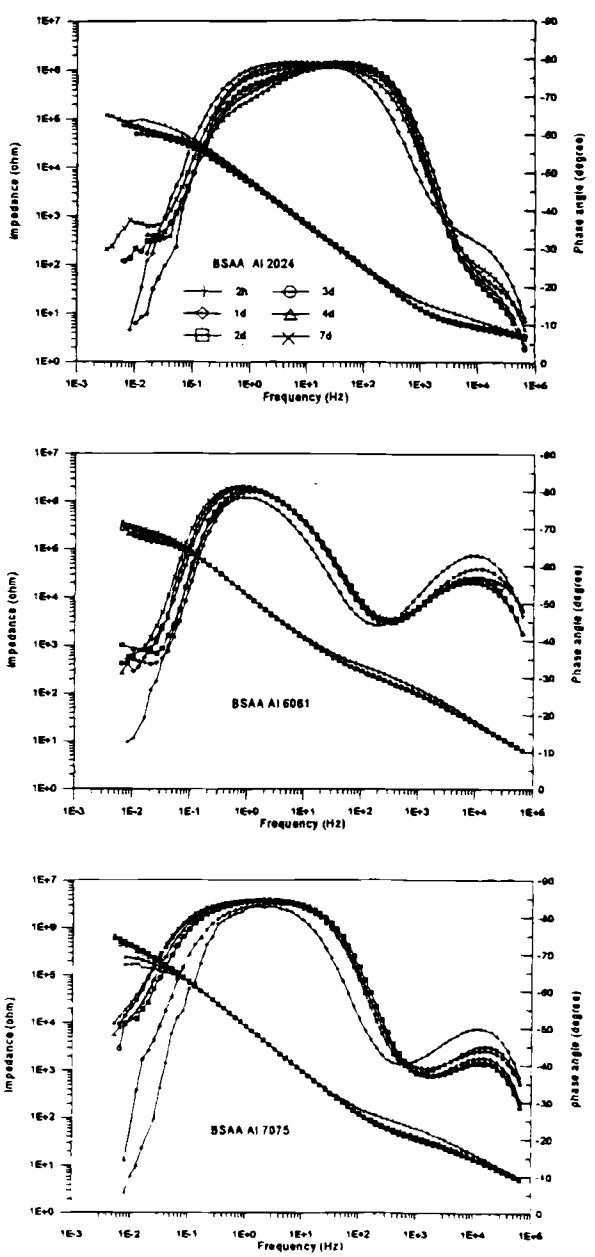

Fig. 2. Impedance spectra for BSAA Al 2024, AL 6061, and Al 7075 sealed in cerium nitrate for 30 min.

Downloaded on 2017-02-21 to IP 149.157.61.151 address. Redistribution subject to ECS terms of use (see ecsdl.org/site/terms_use) unless CC License in place (see abstract).

layer were closed with cerium hydroxide. For Al 2024, the resistance R_{po} of the pores in the outer oxide layer was very low, and therefore the time constant corresponding to the sealed outer porous layer could not be resolved clearly at the highest frequencies. The impedance spectra for all three alloys were very stable with time and after 1 week immersion the pitted area was very small.

The impedance spectra for BSAA Al 2024, Al 6061, and Al 7075 sealed in yttrium chloride are shown in Fig. 3. For Al 2024 and Al 7075, the spectra showed one time constant throughout the entire immersion period similar to sealing in chromate (Fig. 1b) and a very low R_{po}. The spectra for Al 6061 had two time constants with an R_{po} value of $2 \times 10^5\ \Omega\ cm^2$ which is commonly accepted as the standard value for properly HWS Al alloys.[16] All impedance spectra were very stable with time and no occurrence of pitting was indicated in the low-frequency region. After sealing in YCl_3, a large number of tiny pits was detected. This result might be due to the treatment in hot YCl_3, where Cl^- attacked weak spots in the oxide film. Nevertheless, not more than one or two small pits were formed during immersion in 0.5 N NaCl.

The impedance spectra for BSAA Al 2024, Al 6061, and Al 7075 sealed in 50 mM yttrium sulfate at pH 6 for 30 min all contained two time constants (Fig. 4) throughout the 2 week immersion period suggesting that the pores of the porous layer were closed by yttrium oxides/hydroxides. All three BSAA Al alloys exhibited excellent corrosion resistance. After immersion in NaCl for two weeks, no pits were found on Al 6061 and only a very small A_{pit} value was determined for Al 2024 and Al 7075 (Table I).

The time dependence of R_{po} obtained by analysis of the experimental impedance spectra with the software described elsewhere[14,15] for BSAA Al 2024, Al 6061, and Al 7075 sealed by different processes for which two time constants appeared in the impedance spectra is shown in Fig. 5. For HWS Al 2024, the R_{po} values decreased by about a factor of ten from about $5 \times 10^3\ \Omega\ cm^2$ during 1 week immersion indicating dissolution of the porous oxide layer (Fig. 5a). For NiF_2 sealing R_{po} remained at about $1 \times 10^5\ \Omega\ cm^2$ throughout the entire exposure period. For the two cerium nitrate sealing methods, R_{po} was less than $1 \times 10^3\ \Omega\ cm^2$ and decreased slightly with time. For yttrium sulfate sealing I R_{po} was very low in the beginning of immersion, but

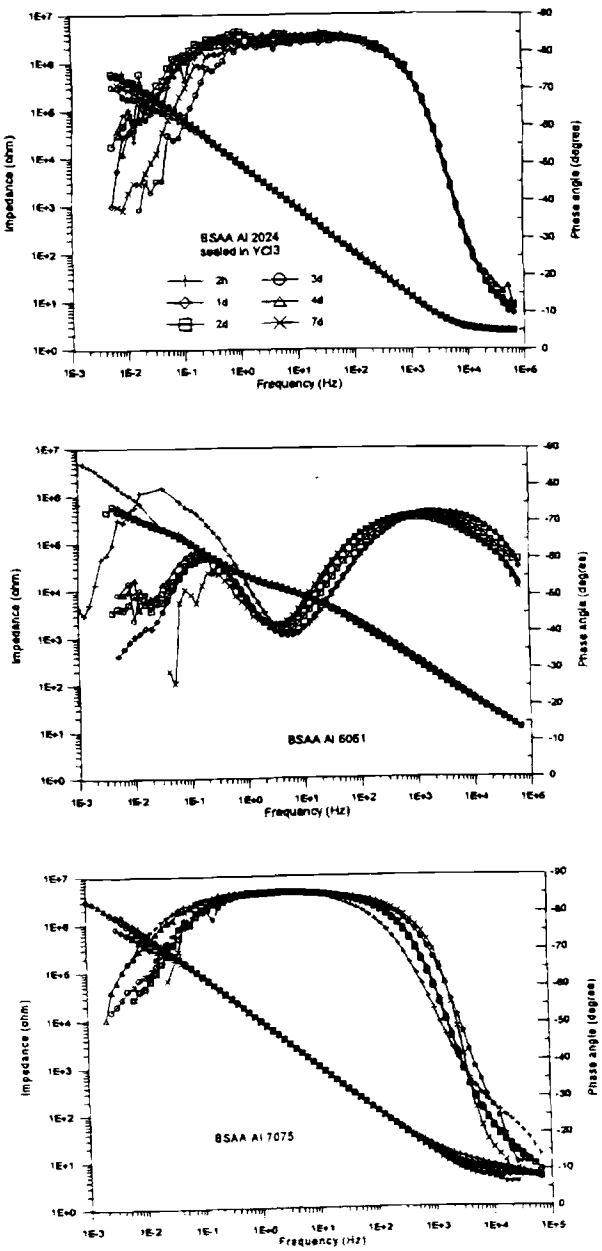

Fig. 3. Impedance spectra for BSAA Al 2024, Al 6061, and Al 7075 sealed in yttrium chloride.

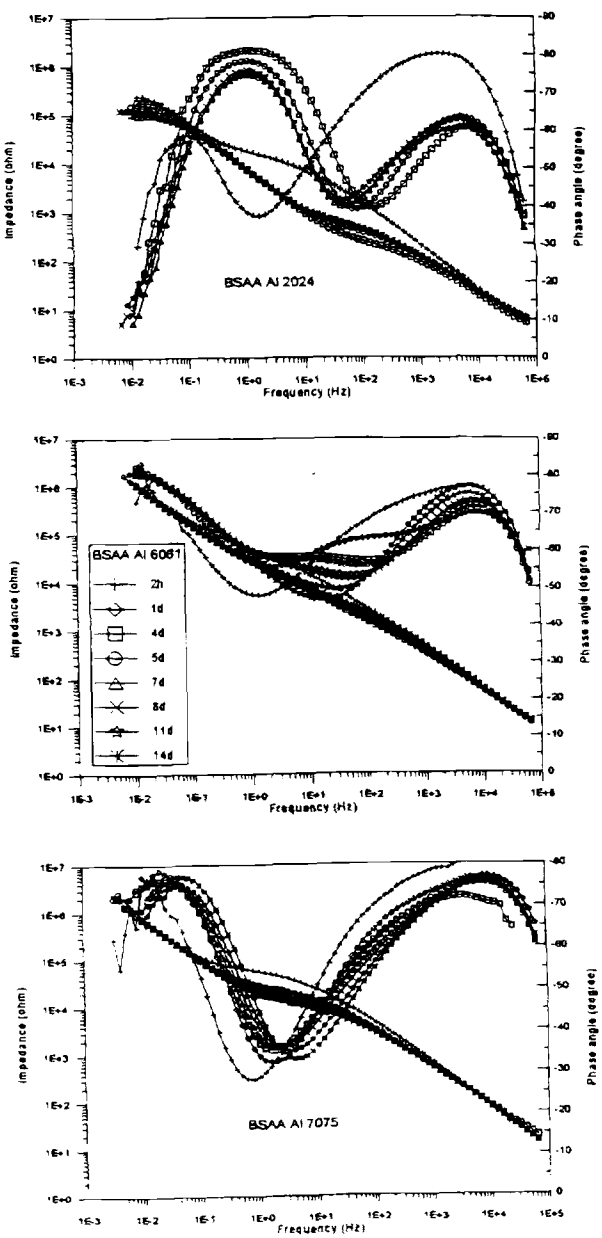

Fig. 4. Impedance spectra for BSAA Al 2024, Al 6061, and Al 7075 sealed in 50 mM yttrium sulfate, pH 6 for 30 min.

Downloaded on 2017-02-21 to IP 149.157.61.151 address. Redistribution subject to ECS terms of use (see ecsdl.org/site/terms_use) unless CC License in place (see abstract).

Table I. Pitted area fraction *F* (%) for BSAA Al alloys after exposure to 0.5 N NaCl for 7 days.

Sealing process	Al 2024	Al 6061	Al 7075
Unsealed	3[a]	0.05	2[a]
Dilute chromate	0	0.001	0
Cold NiF_2	0.001	0.005	0.005
Hot water	0.07	0.05	0.06
$Ce(CH_3COO)_3$	0.02	0.01	0.002
$Ce(NO_3)_3$ (I)	0.005	0.005	0.003
$Ce(NO_3)_3$ (II)	0.001	0.003	0.001
$Ce(CH_3COO)_3 + Ce(NO_3)_3$	0.05	0.03	0.02
$Ce_2(SO_4)_3$	0.02[b]	0.02[b]	0.002[b]
$Ce(SO_4)_2$ (I)	5[b]	0.002[b]	0.004[b]
$Ce(SO_4)_2$ (II)	0.01	0.001[b]	0.002
YCl_3	0.03	0.02	0.004
$Y(CH_3COO)_3$	0.2	0.1	0.01
$Y_2(SO_4)_3$ (I)	0.001	0.003	0.005
$Y_2(SO_4)_3$ (II)	0.001[b]	0[b]	0.001[b]

[a] 3 days.
[b] 14 days.

increased with immersion time due to self-sealing of the porous layer. The sample sealed by yttrium sulfate sealing II had the highest initial R_{po} values which decreased during the first days of immersion, but then reached a constant value of about 10^4 Ω cm^2.

The HWS BSAA Al 6061 sample had relatively stable R_{po} values of about 4×10^4 Ω cm^2 (Fig. 5b). Contrary to the results obtained for BSAA Al 2024 (Fig. 5a) and Al 7075 (Fig. 5c) R_{po} for the nickel fluoride sealed sample was very low initially, but increased with immersion time due to self-sealing. For the two cerium nitrate sealing processes, the R_{po} values were more than one order higher than those for Al 2024 (Fig. 5a) and decreased only slightly with time (Fig. 5b). Similar to Al 2024, yttrium sulfate sealing I produced rapidly increasing R_{po} values with time due to self-sealing. The yttrium sulfate II sealed BSAA Al 6061 sample had the highest R_{po} which decreased slightly with time.

The yttrium sulfate II sealed BSAA Al 7075 sample had the highest R_{po} values which did not change much with time (Fig. 5c). Nickel fluoride sealed sample also had very high R_{po} values comparable to those usually observed for sulfuric acid anodized HWS sealed Al alloys with an oxide layer thickness of about 20 μm.[15] R_{po} for HWS Al 7075 gradually decreased with time, while cerium nitrate I sealed Al 7075 had smaller, but quite stable R_{po} values. Cerium nitrate sealed sample initially had similar R_{po} values, but R_{po} for cerium nitrate II sealed samples decreased with time (Fig. 5c). For yttrium sulfate sealing I R_{po} increased with immersion time similar to Al 2024 and Al 6061 due to self-sealing. The very large differences observed for the two yttrium sulfate sealing methods in Fig. 5 points to significant effects of concentration, pH, and immersion time which are being investigated at present. Sealing in acetate solutions did not produce satisfactory results most likely due to the aggressive nature of these solutions.

The specific admittance A_s is defined as the inverse of the impedance modulus $|Z|$ determined at 1 kHz and normalized to the exposed area.[7,16] For sealed, anodized Al alloys A_s depends on the value of R_{po} as shown in Fig. 6. The two curves were calculated for the equivalent circuit commonly used for anodized Al alloys shown in Fig. 6 using a barrier layer thickness d_b = 100 Å and a porous oxide layer thickness d_p = 1 μm to simulate the behavior of BSAA Al alloys (curve 1) and d_b = 200 Å and d_p = 20 μm for HWS sulfuric acid anodized Al alloys (curve 2). For very high values of R_{po}, A_s is related to the capacitance C_p of the porous layer, while for very low values of R_{po} it is related to the capacitance C_b of the barrier layer. In these two limiting cases, $A_s = 2\pi fC = 2000\ \pi\epsilon\epsilon_0/d$ is related to the thickness d of the oxide layer, which is the porous oxide layer when the pores are sealed (i.e., in HWS where R_{po} is high), and the barrier layer when the pores are not sealed (i.e., in chromate sealing) and R_{po} is low.[7,16] An increase of A_s indicates a decrease of d at constant ϵ (Fig. 6). For a barrier layer with d_b = 100 Å and $\epsilon_b = 10$, $A_s = 5.6 \times 10^3$ μS/cm^2, while for a porous layer with d_p = 1 μm and $\epsilon_p = 50$, A_s = 278 μS/cm^2 which are the two limits of A_s for curve 1 in Fig. 6. The straight line with a slope close to −1 between these two limits is independent of d_b and d_p. Determination of A_s provides a convenient means of qualitative evaluation of oxide properties and their changes with exposure time without the need for detailed data analysis of the impedance spectra provided that A_s does not fall into the transition region shown in Fig. 6 for $10^2 < R_{po} < 10^4$ Ω cm^2.

Figure 7 and 8 show the time dependence of A_s for BSAA Al 2024, Al 6061, and Al 7075 sealed with various cerium salt (Fig. 7) and yttrium salt (Fig. 8) solutions. For unsealed BSAA Al 2024 and Al 7075, the A_s values were initially characteristic of the capacitance C_b of the barrier layer and then increased with immersion time indicating dissolution of the oxide layer. For Al 6061, A_s values were close to 350 μS/cm^2, which is equivalent to an oxide thickness of 1 μm, and remained relatively stable with time (Fig. 7b). For all three chromate sealed BSAA samples, A_s had the values calculated from d_b and remained almost

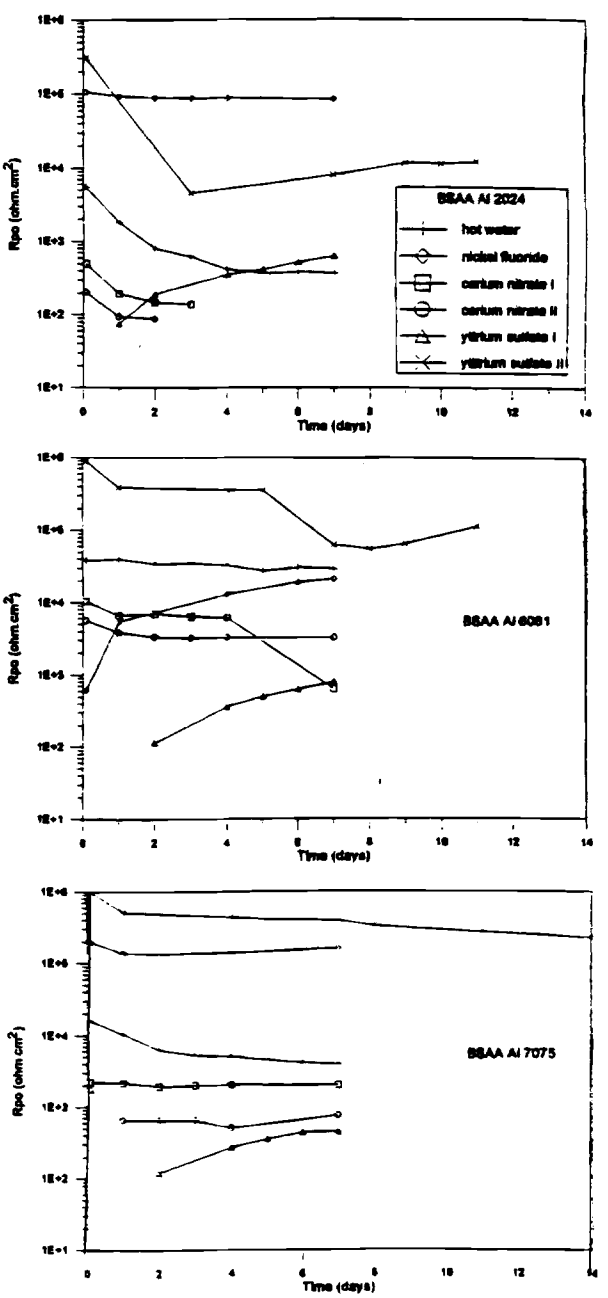

Fig. 5. Time dependence of the pore resistance R_{po} for sealed BSAA Al alloys.

Downloaded on 2017-02-21 to IP 149.157.61.151 address. Redistribution subject to ECS terms of use (see ecsdl.org/site/terms_use) unless CC License in place (see abstract).

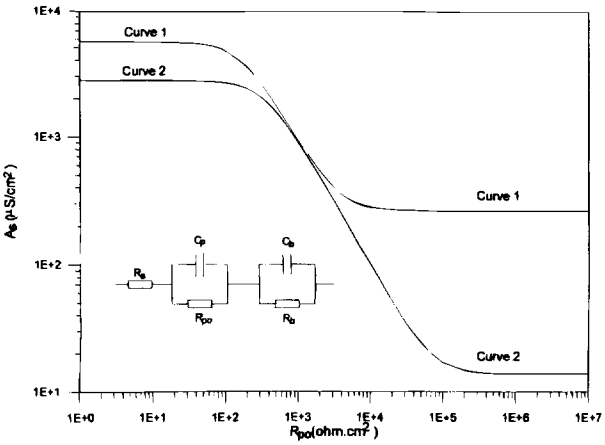

Fig. 6. Theoretical relationship between the specific admittance A_s and the pore resistance R_{po}; curve 1: d_b = 100 Å, d_p = 1 μm; curve 2: d_b = 200 Å, d_p = 20 μm.

constant throughout the 1 week immersion period. For HWS, the A_s values were low corresponding to d_p, but increased with immersion time due to dissolution of the porous layers. The A_s values for cold nickel fluoride sealed Al 2024 and Al 7075 had values close to those calculated for a porous layer of about 1 μm thickness and were very stable with time, while for Al 6061 A_s decreased with time due to self-sealing of the porous layer. This result reflects the observation that the sealing mechanism for BSAA Al 6061 is often different from that for the other two alloys.

For BSAA Al 2024 sealed in cerium acetate, the A_s values increased continuously with exposure time due to dissolution of the oxide layer (Fig. 7a). For sealing in the cerium nitrate solutions I and II, the A_s values were high and determined mainly by C_b since R_{po} was low (Fig. 5 and 6). For sealing in cerium acetate followed in cerium nitrate, A_s values were high and increased sharply with time. For sealing in cerium (III) sulfate, A_s values were high at first indicating that the porous layer was not sealed, however, A_s decreased slowly with time due to the self-sealing of the

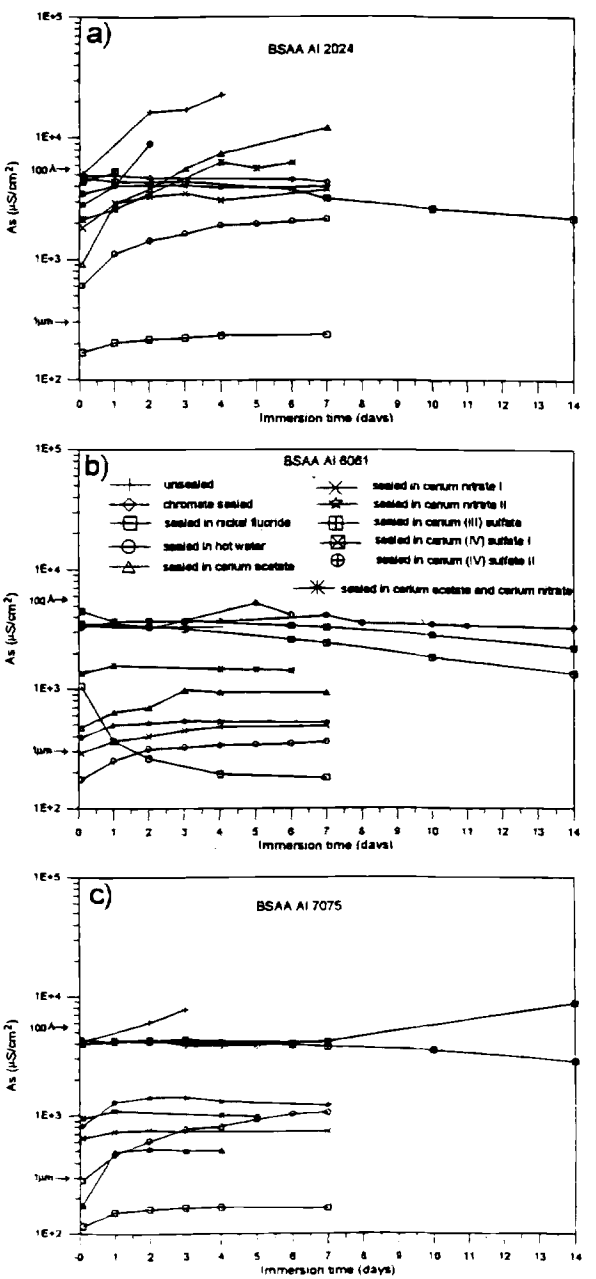

Fig. 7. Time dependence of the specific admittance A_s for BSAA Al alloys sealed in cerium salt solutions.

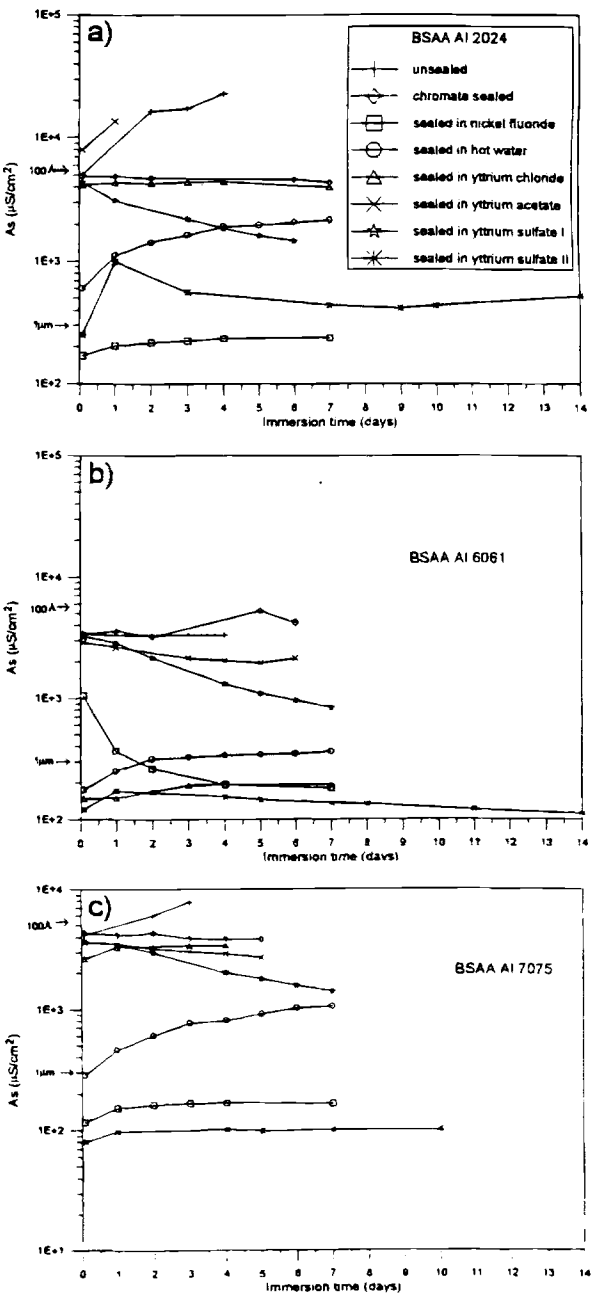

Fig. 8. Time dependence of the specific admittance A_s for BSAA Al alloys sealed in yttrium salt solutions.

Downloaded on 2017-02-21 to IP 149.157.61.151 address. Redistribution subject to ECS terms of use (see ecsdl.org/site/terms_use) unless CC License in place (see abstract).

porous outer oxide layer during immersion in 0.5 N NaCl. The A_s values for both cerium (IV) sulfate sealing solutions were high and increased sharply with immersion time indicating poor sealing efficiency (Fig. 7).

For Al 6061 sealed in cerium acetate, cerium nitrate I and II, the A_s values were low corresponding to C_p and increased slightly at the beginning of immersion. The A_s values for sealing in cerium(III) sulfate were high, but decreased with time indicating that the pores in the outer oxide layer was self-sealing during immersion in 0.5 N NaCl. The samples sealed in cerium(IV) sulfate I and II had high A_s value characteristic of C_b (Fig. 7). For Al 7075, cerium(III) sulfate sealing as well as cerium(IV) sulfate I and II sealing produced very similar results with high A_s values as expected for the barrier oxide layer. For all the other sealing procedures, A_s values were lower corresponding to C_p and were quite stable with time (Fig. 7).

For BSAA Al 2024 sealed in yttrium chloride, the A_s values were high and stable with time similar to those of the chromate sealed sample (Fig. 8a). Yttrium acetate sealed BSAA Al 2024 had very high A_s values which increased with time due to the dissolution of the oxide layer. For the yttrium sulfate sealing process I, A_s was initially quite high similar to the value for yttrium chloride and chromate sealed samples, but decreased steadily with the exposure time. This indicated that the outer porous layer was not sealed in the first stages of exposure, but became sealed during immersion in 0.5 N NaCl. For the yttrium sulfate sealing process II, which had a different pH solution and longer sealing time, the A_s values were low as calculated for C_p and quite stable with time.

The A_s values for sealed BSAA Al 6061 fell into two groups (Fig. 8b). The yttrium acetate and yttrium sulfate I sealed Al 6061 samples had high A_s values corresponding to C_b similar to unsealed and chromate sealed samples, while the HWS, the yttrium chloride and yttrium sulfate II sealed samples had low A_s values according to C_p (Fig. 8b). The A_s values for the yttrium sulfate I sealed sample decreased with time indicating that self-sealing occurred in the NaCl solution. The yttrium sulfate sealing process II produced the lowest A_s values which were stable with time. The time dependence of A_s for BSAA Al 6061 sealed in nickel fluoride was different from that for the other two alloys. A_s decreased continuously from an initial value of 1000 to about 200 $\mu S/cm^2$ observed for BSAA Al 2024 and 7075. For Al 7075 sealed in yttrium chloride, the A_s values were high and close to those for the chromate sealed sample. A_s increased in the beginning of immersion and became stable after 1 day. For sealing in yttrium acetate and yttrium sulfate I, the A_s values were also high, but decreased with time due to self-sealing. For the yttrium sulfate sealing process II, very low A_s values were observed corresponding to a porous layer thickness exceeding 1 μm (Fig. 8c).

A test of the theoretical prediction of the relationship between A_s and R_{po} given in Fig. 6 has been made by plotting the experimental values of A_s in Fig. 7 and 8 as a function of the experimental values of R_{po} for those alloys and sealing solutions for which two time constants were observed. Although there is some scatter in the data, Fig. 9 shows that the results for Al 7075 and Al 2024 are close to the theoretical relationship calculated in Fig. 6 for BSAA Al alloys. For Al 2024 a more or less constant value of A_s occurs at the highest and lowest values of R_{po} (Fig. 9). No explanation can be given at present for the finding that the results for Al 6061 are shifted to lower values of R_{po} for a given value of A_s. However, these results confirm the finding that BSAA Al 6061 behaved differently than the other two alloys. The results in Fig. 9 suggest that for some alloy/sealing combinations both A_s and R_{po} changed during exposure to 0.5 N NaCl. For samples with poor corrosion resistance A_s increased as the oxide layer became thinner and R_{po} decreased, while for samples for which self-sealing occurred R_{po} increased accompanied by a decrease of A_s.

Table I lists the pitted area fraction $F = A_{pit}/A_t$ determined at the end of exposure for the different sealing treatments, where A_t is the total exposed area. Sealing in dilute

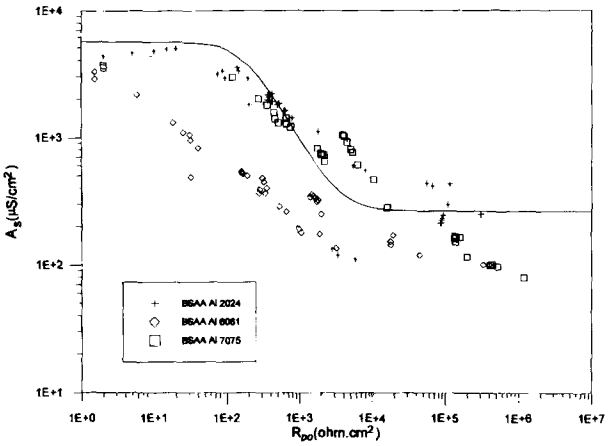

Fig. 9. Dependence of the experimental values of the specific admittance A_s on the pore resistance R_{po} for sealed BSAA Al alloys.

chromate, which is the procedure used at Boeing, and sealing in cold nickel fluoride produced excellent results, while the corrosion resistance of the HWS sealed samples was poor. Sealing in the two cerium nitrate solutions produced surfaces with a corrosion resistance comparable to that of the chromate or nickel fluoride sealed samples. Sealing in the two cerium sulfate solutions produced very good results for Al 7075 and to some extent for Al 6061, but was not as effective for Al 2024 (Table I). Despite the fact that BSAA samples were covered with a large number of very small pits after sealing in YCl_3, excellent corrosion resistance was observed during immersion in NaCl especially for Al 7075. Table I lists the total F value including the pitted area due to sealing in YCl_3. Sealing in yttrium sulfate produced very corrosion resistant surfaces, especially when higher concentrations and longer sealing times were used. Poor results were obtained for sealing in solutions containing acetate which seem to be too corrosive. The difficulties in effectively sealing BSAA Al 2024 become apparent from the results in Table I, where the highest values of A_{pit} were usually found for this material.

Table II list the specific pit resistance R°_{pit} which is proportional to the pit growth rate for sealed BSAA Al alloys determined after 1 week immersion. R°_{pit} was calculated from the experimental values of R_{pit} obtained from analysis of the impedance spectra and A_{pit} obtained by visual observation (Table I) as $R^\circ_{pit} = R_{pit} \times A_{pit}$. [13,14] Each alloy had a relatively constant pit growth rate independent of the sealing method. BSAA Al 2024 had the fastest and Al 6061 had the lowest pit growth rate in agreement with the known corrosion behavior of these alloys. Once pits have penetrated the oxide layer, only the bulk alloy properties and not the oxide layer properties determine pit growth rates. Pit growth rates calculated from R°_{pit} were about 5 mm/year for BSAA Al 2024, 0.8 mm/year for Al 6061, and 2 mm/year for Al 7075.

Summary and Conclusions

The corrosion resistance of three BSAA Al alloys sealed in different cerium and yttrium solutions has been evaluated by recording of impedance spectra during immersion in

Table II. Specific pitting resistance [R°_{pit} (Ω cm²] for sealed BSAA Al alloys.

Sealing process	Al 2024	Al 6061	Al 7075
Hot water	49	300	120
$Ce(CH_3COO)_3$	40	200	n.p.
$Ce_2(SO_4)_3$	40	240	n.p.
$Ce(SO_4)_2$ (II)	40	n.p.	n.p.
$Ce(CH_3COO)_3$ + $Ce(NO_3)_3$	50	240	100
$Y(CH_3COO)_3$	40	240	100

n.p.: no pits.

Downloaded on 2017-02-21 to IP 149.157.61.151 address. Redistribution subject to ECS terms of use (see ecsdl.org/site/terms_use) unless CC License in place (see abstract).

0.5 N NaCl and by visual observation at the end of the exposure test. Comparisons have been made with results obtained with presently used sealing methods such as hot water sealing and sealing in dilute chromate or cold nickel fluoride. Sealing in dilute chromate, the process used at present for BSAA Al alloys, produced excellent corrosion resistance. The impedance spectra suggested that in this sealing process the pores stayed open and are apparently filled with Cr^{6+} acting as inhibitor. On the other hand, the pores became plugged with oxide/hydroxide during hot water sealing and sealing in cold nickel fluoride. Sealing in different cerium or yttrium solutions occurred according to one of these two mechanisms depending on the alloy type and solution characteristics. The corrosion resistance of HWS BSAA Al alloys was poor most likely due to the relatively thin oxide layers of about 1 μm thickness. The best results for all three BSAA alloys were obtained for sealing in cerium nitrate and yttrium sulfate solutions. For sealing in cerium nitrate very stable impedance spectra were determined with a relatively low pore resistance R_{po}. When sealing in yttrium sulfate for 15 min, impedance spectra were similar to those for sealing in chromate, however R_{po} increased slowly with exposure time due to self-sealing. Much higher R_{po} values were obtained when the concentration of yttrium sulfate and the sealing time were increased.

For sulfuric acid anodized and HWS Al alloys with an oxide thickness of 20 μm a R_{po} value exceeding 2×10^5 Ω cm^2 has been suggested as a criterion for efficient sealing.[16] Assuming that R_{po} decreases linearly with oxide thickness, the critical R_{po} value for BSAA alloys would be about 10^4 Ω cm^2. Sealing in yttrium sulfate II resulted in R_{po} values exceeding this critical value for all three BSAA Al alloys. The same result was obtained for nickel fluoride sealed Al 2024 and Al 7075, while for Al 6061 self-sealing occurred with R_{po} exceeding the threshold value after about 3 days (Fig. 5). For HWS BSAA Al 6061 and Al 7075 initial R_{po} values exceeded 10^4 Ω cm^2, while for BSAA Al 2024 R_{po} decreased continuously. In considering these results, which point out possible effects of alloy composition and sealing bath chemistry, it has to be considered that R_{po} by itself is not a quantitative measure of sealing quality although it is an indicator of the sealing mechanism. Sealing in dilute chromate produced excellent corrosion resistance (Table I), but resulted in very low R_{po} values since the pores remained open. For BSAA Al 7075, F = 0.001% was determined for sealing in cerium nitrate II and in yttrium sulfate II (Table I), however R_{po} was less than 10^3 Ω cm^2 for the former treatment and exceeded 10^5 Ω cm^2 for the latter.

As discussed by Otero et al.,[16] the use of A_s has been proposed as a measure of the quality of the hot water sealing process of sulfuric acid anodized Al alloys. For an adequately sealed Al alloy with an oxide thickness d = 20 μm and ϵ_p = 36, A_s has to be equal or less than 10 μS/cm^2. [16] In this context it is important to note that A_s depends on the oxide thickness d and dielectric constant ϵ, which are not changed significantly by sealing. The reason for the changes of A_s with sealing and subsequent aging treatments observed by Otero et al.[16] are the changes of A_s with R_{po} illustrated in Fig. 6. As the porous oxide became fully sealed, A_s decreased to a constant value of about 10 μS/cm^2 similar to the changes shown in Fig. 6. Similar results were observed in the present study, where sealed samples for which self-sealing occurred during exposure to NaCl showed an increase of R_{po} accompanied by a decrease of A_s, while for samples with poor corrosion resistance, for which A_s increased as the oxide layer thickness decreased, R_{po} decreased with time (Fig. 9). Care with the use of A_s as a criterion for sealing quality must be therefore exercised since it depends on the anodizing process, which affects the value of d, and on the actual value of R_{po}. As shown in Fig. 9 the results obtained for BSAA Al 2024 and Al 7075 were in general agreement with the model, however, the results for Al 6061 showed a different relationship between A_s and R_{po} confirming the observation that in many cases Al 6061 had a different response to a given sealing process than the other two alloys.

BSAA Al 6061 and Al 7075 sealed in cerium nitrate II or yttrium sulfate II passed the salt spray test, while for Al 2024 the observed number of pits was slightly too high. Certain modifications of the present sealing treatments for Al 2024 are being evaluated at present using factorial design experiments. Paint adhesion was excellent for all three alloys and both sealing solutions. The excellent corrosion resistance observed for the three Al alloys treated in the BSAA process and sealed in certain REMS solutions suggests that these new sealing procedures show promise as replacements of the dilute chromate solution used at present.

Acknowledgment

The authors acknowledge financial support and the supply of BSAA Al alloys from Boeing Information, Space and Defense Systems.

Manuscript submitted September 12, 1997; revised manuscript received February 17, 1998.

The University of Southern California assisted in meeting the publication costs of this article.

REFERENCES

1. B. Yaffe, Met. Finish., **88**, 41 (1990).
2. A. Dito and F. Tegiacchi, *Plat. Surf. Finish.*, **72**, 72 (1985).
3. M. R. Kalantry, D. R. Gabe, and D. H. Ross, Plat. Surf. Finish., **78**, 24 (1991).
4. M. R. Kalantry, D. R. Gabe, and D. H. Ross, *Plat. Surf. Finish.*, **80**, 52 (1993).
5. P. Haudrechy, J. Foussereau, B. Mantout, and B. Baroux, *Contact Dermatitis*, **31**, 249 (1994).
6. NASA Tech Briefs (May 1995).
7. F. Mansfeld, G. Zhang, and C. Chen, *Plat. Surf. Finish.*, **84**,72 (1997).
8. *Anodizing of Aluminum Alloys*, Boeing Process Spec. 5632.
9. F. Mansfeld and Y. Wang, *Br. Corros. J.*, **29**, 194 (1994).
10. F. Mansfeld and Y. Wang, *Mater. Sci. Eng.*, **198A**, 51 (1995).
11. U.S. Pat. 5,194,138 (1993).
12. U. S. Pat. 5,582,654 (1996).
13. C. Chen, Ph.D. Thesis, University of Southern California, Los Angeles, CA (1997).
14. F. Mansfeld, C. H. Tsai, and H. Shih, *ASTM STP*, **1154**, 186 (1992).
15. F. Mansfeld, Y. Wang, S. H. Lin, H. Xiao, and H. Shih, *ASTM STP*, **1188**, 37 (1993).
16. E. Otero, V. Lopez, and J. A. Gonzalez, *Plat. Surf. Finish.*, **83**, 50 (1996).

Downloaded on 2017-02-21 to IP 149.157.61.151 address. Redistribution subject to ECS terms of use (see ecsdl.org/site/terms_use) unless CC License in place (see abstract).